DEUTSCHES ELEKTRONEN-SYNCHROTRON DESY

DESY 83-035
May 1983

MEASUREMENT OF THE PROCESSES $e^+e^- \to e^+e^-$ AND $e^+e^- \to \gamma\gamma$ AT PETRA

by

JADE Collaboration

ISSN 0418-9833

NOTKESTRASSE 85 · 2 HAMBURG 52

To be sure that your preprints are promptly included in the
HIGH ENERGY PHYSICS INDEX ,
send them to the following address (if possible by air mail) :

DESY
Bibliothek
Notkestrasse 85
2 Hamburg 52
Germany

DESY 83-035
May 1983

ISSN 0418-9833

Measurement of the processes $e^+e^- \to e^+e^-$ and $e^+e^- \to \gamma\gamma$ at PETRA

JADE Collaboration

W. Bartel, L. Becker, C. Bowdery, D. Cords, R. Eichler[1], R. Felst, D. Haidt, H. Krehbiel, B. Naroska, J. Olsson, P. Steffen, P. Warming

Deutsches Elcktronen-Synchrotron DESY, Hamburg, Germany

G. Dietrich, E. Elsen[2], G. Heinzelmann, H. Kado, K. Meier, A. Petersen, U. Schneekloth, G. Weber

II. Institut für Experimentalphysik, Universität Hamburg, Germany

S. Bethke, A. Dieckmann, J. Heintze, K.H. Hellenbrand, R.D. Heuer, S. Komamiya, J. von Krogh, P. Lennert, H. Matsumura, H. Rieseberg, A. Wagner[3]

Physikalisches Institut der Universität Heidelberg, Germany

A. Bell[4], A, Finch, F. Foster, G. Hughes, T. Nozaki, H. Wriedt

University of Lancaster, England

J. Allison, A.H. Ball, G. Bamford, R. Barlow, I.P. Duerdoth, I. Glendinning, F.K. Loebinger, A.A. Macbeth, H. McCann, H.E. Mills, P.G. Murphy, P. Rowe, K. Stephens

University of Manchester, England

D. Clarke, R. Marshall, G.F. Pearce, J.B. Whittaker

Rutherford Appleton Laboratory, Chilton, England

J. Kanzaki, T. Kawamoto, T. Kobayashi, M. Koshiba, M. Minowa, M. Nozaki, S. Odaka, S. Orito, A. Sato, H. Takeda, T. Takeshita, Y. Totsuka, Y. Watanabe[5], S. Yamada, C. Yanagisawa[6]

Lab. of Int. Coll. on Elementary Particle Physics
and Department of Physics, University of Tokyo, Japan

[1] now at Labor f. Hochenergiephysik der ETH-Zurich, Villigen, Switzerland

[2] now at SLAC, California, U.S.A.
[3] Heisenberg Foundation Fellow
[4] now at British Petroleum, London, England
[5] now at KEK, Oho-machi, Tsukuba-gun, Ibaraki-ken, Japan
[6] now at Rutherford Appleton Laboratory, Chilton, England

Abstract

Cross sections for the reactions $e^+e^- \to e^+e^-$ (Bhabha scattering) and $e^+e^- \to \gamma\gamma$ are measured for center-of-mass (c.m.) energies $\sqrt{s}$ between 12.0 and 34.6 GeV. The results agree with the predictions of Quantum Electrodynamics (QED) and the cut-off parameters are determined. From Bhabha scattering at the highest energy, $\langle\sqrt{s}\rangle = 34.6$ GeV, the 1σ limits $0.12 < \sin^2\vartheta_w < 0.38$ are obtained for the weak mixing angle. The higher order (α^3) QED processes $e^+e^- \to e^+e^-\gamma$ and $e^+e^- \to \gamma\gamma\gamma$ are also studied and are found to agree with the α^3 QED predictions. A search for excited electrons is carried out by investigating the $(e^\pm\gamma)$ invariant mass distribution in the reaction $e^+e^- \to e^+e^-\gamma$.

The lowest order QED processes $e^+e^- \to e^+e^-$ and $e^+e^- \to \gamma\gamma$ have already been studied at PETRA energies /1,2/. In this letter, we report on the measurements of these reactions with higher statistics at c.m. energies between 12.0 GeV and 34.6 GeV. The reaction $e^+e^- \to \gamma\gamma$ provides a clean test of QED, since it is free from electro-weak effects in lowest order. On the other hand, Bhabha scattering becomes sensitive to weak interaction effects for $\sqrt{s} > 30$ GeV. The radiative corrections of order α^3 amount to several percent in the present analysis of the lowest order QED processes. The higher order QED processes $e^+e^- \to e^+e^-\gamma$ and $e^+e^- \to \gamma\gamma\gamma$ are also analysed in order to check the validity of the radiative corrections.

The experiment was carried out with the JADE detector at the e^+e^- colliding machine PETRA at DESY. The JADE detector has been described previously/1,3/. For the present analysis, the essential part of the detector is an array of 2712 lead-glass shower counters which covers the polar angle regions $|\cos\vartheta| \leq 0.82$ (barrel) and $0.89 \leq |\cos\vartheta| \leq 0.97$ (end-caps). The fractional energy resolution of the barrel shower counters is 2 % for Bhabha events at $\sqrt{s} = 34$ GeV. The barrel counters were used in the analysis of the cross sections, the normalisation being obtained from Bhabha scattering in the end-cap counters. The cylindrical drift chamber (jet chamber) inside the lead-glass array was used to distinguish photons from electrons/positrons and to discriminate between electrons and

positrons by measuring their curvatures in the axial magnetic field of 4.8 kG.

The data reported here were accumulated between autumn 1979 and autumn 1982, the total integrated luminosity being 75.7 pb^{-1}. The major part of the data, 68.9 pb^{-1}, was taken at high energies, $\sqrt{s} \geq 32$ GeV. The QED events under study were recorded using the shower energy trigger, which required the detection of more than 4 GeV (2 GeV) in the lead-glass for $\sqrt{s} \geq 20$ GeV ($\sqrt{s} \leq 20$ GeV). The selection criteria for the events $e^+e^- \to e^+e^-$ and $\gamma\gamma$ in the barrel part were as follows:

1) At least two clusters of shower energy were required in the lead-glass, each having more than one third of the beam energy;
2) The acollinearity angle between the two shower clusters was required to be less than 10 °;
3) Both clusters had to be in the fiducial volume defined by $|\cos\vartheta| \leq 0.76$.

If there were more than two energetic shower clusters, all pairs were subjected to the above criteria and the event was accepted if any one of them satisfied the criteria. In total, 100316 events were selected by the above criteria. The $\gamma\gamma$ events were then identified by requiring that at least one of the energetic clusters was not connected to any charged track in the jet chamber. (Such clusters are later referred to as 'neutral' clusters.)

In order to purify the sample, we visually inspected those events which had a large number of charged tracks and those where the connection between charged tracks and big shower clusters was bad. Thus, 3.6 % of the events which passed the criteria 1)-3) above were scanned and 37 % of these scanned events were rejected. The rejected events were mostly $e^+e^- \to$ hadrons, $\tau^+\tau^-$ and $e^+e^-\gamma$. In the $e^+e^-\gamma$ case, one of the clusters in the selected pair was due to the photon while the other was due to the electron or positron. After this procedure, 88355 events were classified as $e^+e^- \to e^+e^-$ and 10627 as $e^+e^- \to \gamma\gamma$. The remaining backgrounds were estimated by applying the same selection procedure to Monte Carlo simulated events /4,5/. Hadronic background was negligibly small (< 0.01 % of the e^+e^- events). Background from $e^+e^- \to \tau^+\tau^-$ was estimated to be 0.1 % at $\sqrt{s}$ = 30 GeV and was subtracted statistically from the e^+e^- events. The process $e^+e^- \to e^+e^-\gamma$ contaminated both the e^+e^- and $\gamma\gamma$ final states as follows: Events in which an energetic photon was emitted very close to the electron or positron direction faked the process $e^+e^- \to e^+e^-$, even though the pair consisting of the electron and positron clusters would not have satisfied the above criteria; this contamination accounted for 0.3 % of

the selected e^+e^- events at $\sqrt{s}$ = 30 GeV. Events in which the electron and positron were very close to each other and opposite to a high energy photon faked the process $e^+e^- \to \gamma\gamma$ with one photon converted; we estimated that 2 % of the selected $\gamma\gamma$ events were due to this process. Backgrounds from cosmic rays were found to be negligibly small in the selected events.

Small corrections have been made to the data to allow for dead lead glass counters (< 1 %), uncertainty in the absolute shower energy (< 1 %) and losses due to small gaps between the lead glass counters in the azimuthal angle (< 2 %).

Since we allowed at most one photon to convert to an e^+e^-pair in the material of the beam pipe or the jet chamber, we have to make a further correction for those $\gamma\gamma$ events where both photons convert. The original number of $\gamma\gamma$ events was calculated statistically from the observed numbers of non-converted and singly-converted $\gamma\gamma$ events for each angular bin.

Fig. 1 shows the cross sections for the reaction $e^+e^- \to \gamma\gamma$; Fig. 1-a shows the total cross section in the region $|\cos\vartheta| \leq 0.76$ while Fig. 1-b shows the differential cross sections at $\sqrt{s}$ = 14, 22 and 34.6 GeV. Radiative corrections up to order α^3 /5/ have been applied to the data. The total systematic error on the cross sections was typically 3.2 %, due mainly to the uncertainty in the luminosity determination. The data agree well with the QED predictions. Possible deviations of the data from the QED predictions can be parametrized by the cut-off parameters $\Lambda\pm$/6/ as follows:

$$\frac{d\sigma}{d\Omega} = \frac{\alpha^2}{s}\,\frac{1+x^2}{1-x^2}\left[\,1 \pm \frac{s^2}{2\Lambda\pm^4}\,(1-x^2)\,\right],$$

where $x = \cos\vartheta$.

The data at the highest energy, $\langle\sqrt{s}\rangle$ = 34.6 GeV, were used to obtain the 95 % confidence level lower limits $\Lambda+ > 61$ GeV and $\Lambda- > 57$ GeV . In estimating these limits, the overall normalisation was allowed to vary within the total systematic error on the cross section. The ratio of the measured differential cross section to that of lowest order QED is plotted in Fig.1-c together with the expectations for $\Lambda\pm$ = 50 and 60 GeV.

As was stated previously, the jet chamber was used to distinguish between the final state particles in the reaction $e^+e^- \to e^+e^-$. When a big

shower cluster was connected with more than one charged track, the charge of the highest momentum track was used. In some cases, however, one of the pair was assigned the wrong charge, resulting in a doubly positive or negative pair. This charge mis-assignment was mainly due to showering effects in the beam pipe material, although it was also partly due to the finite momentum resolution of the jet chamber. The probability of charge mis-assignment was typically 4 % and it was corrected statistically for each angular bin.

Doubly converted $\gamma\gamma$ events were subtracted statistically (< 0.3 % of the e^+e^- events). After applying radiative corrections /5/ to the data, we obtain the integrated cross sections for the region $|\cos\vartheta| \leqq 0.76$ which are shown in Fig. 2-a and the differential cross sections shown in Fig.2-b.

There is excellent agreement between the data and the QED predictions. In order to express this agreement in terms of a cut-off parameter Λ, we introduce a hypothetical modification /7/ of the photon propagator $(1/q^2)$ by multiplying it with the form factor

$$F(q^2) = 1 \mp q^2/(q^2 - \Lambda\pm^2),$$

where q^2 is the square of the invariant mass of the virtual photon. Then the differential cross section is given by

$$\frac{d\sigma}{d\Omega} = \frac{\alpha^2}{4s}\left[\frac{10+4x+2x^2}{(1-x)^2}F^2(t) - \frac{2(1+x)^2}{1-x}F(s)F(t) + (1+x^2)F^2(s)\right],$$

where t is the square of the 4-momentum transfer between the incoming and outgoing electron (positron) and is given by $t = -s(1-x)/2$ in the high energy limit.

The 95 % confidence level lower limits on $\Lambda+$ and $\Lambda-$ were found to be 178 GeV and 200 GeV, respectively. In estimating the cut-off parameters, the electro-weak effect was subtracted, assuming $\sin^2\vartheta_w = 0.228$ /8/. Changes in the luminosity due to non-infinite Λ values were taken into account in the χ^2 fit.

Electro-weak interference effects in Bhabha scattering were studied in the context of the standard model, with $\sin^2\vartheta_w$ as the only parameter /9/. As in the study of the cut-off parameters, only the highest energy data were used. The interference effect is rather small in Bhabha scattering. Thus, the fit could only limit the Weinberg angle to the range $0.12 < \sin^2\vartheta_w < 0.38$ at the 68 % confidence level. The effect of the electro-weak

interference on the luminosity determination was taken into account in the χ^2 fit. The ratio of the differential cross section to that of lowest order QED is shown in Fig.2-c together with the prediction of electro-weak interference with $\sin^2\vartheta_w = 0.26$, the value which gives the minimum χ^2 in the above analysis.

Some models /10,11/ differ from the standard electro-weak model in that they predict the existence of two neutral gauge bosons, leading to a modified vector coupling constant of the form

$$v^2 = (1 - 4 \sin^2\vartheta_w)^2 + 16C.$$

The axial coupling is still given by $a^2=1$, as in the standard model.

With $\sin^2\vartheta_w$ fixed to 0.228 /8/, the following upper limit on C was obtained:

$$C < 0.031 \qquad (95\ \%\ \text{C.L.}) .$$

In the above analyses of the lowest order QED processes $e^+e^- \to e^+e^-$ and $\gamma\gamma$, radiative corrections up to order α^3 were applied. To check the validity of the radiative corrections, the higher order QED processes $e^+e^- \to e^+e^-\gamma$ and $\gamma\gamma\gamma$ were studied. The selection criteria for these reactions were as follows:

1. At least three shower clusters were required in the barrel lead glass counters ($|\cos\vartheta| \leqq 0.77$).
   The biggest two clusters (third cluster) should have more than 1/3 (1/10) of the beam energy, and the sum of the three cluster energies should be greater than 75 % of the c.m. energy;
2. The opening angle between any two clusters should be bigger than 10°;
3. The sum of the three opening angles should be greater than 350°.

The last criterion required three body kinematics in the final state and rejected some fraction of $e^+e^-\gamma\gamma$ and $\gamma\gamma\gamma\gamma$ events. When there were more than three clusters, all possible combinations of three clusters were subjected to the above criteria and the event was accepted if any one of them satisfied the criteria. Only one neutral cluster was required for $e^+e^-\gamma$ identification, while at least two neutrals were required for $\gamma\gamma\gamma$ identification. After visual inspection of all the candidate events, 2506 events were selected as $e^+e^-\gamma$ and 193 as $\gamma\gamma\gamma$. After small corrections for inefficiencies, these numbers become 2513 ± 50 and 194.6 ± 14.0 respectively. Doubly converted $\gamma\gamma\gamma$ events were classified as $e^+e^-\gamma$ and

subtracted statistically (0.5 % of the $e^+e^-\gamma$ events). Monte Carlo simulations of these order α^3 QED processes predicted that the corresponding corrected numbers should be 2588 ± 23 and 178.0 ± 4.3, respectively. Various kinematical distributions are shown in Fig. 3 together with the QED predictions; the observed good agreement confirms that the radiative corrections to the lowest order processes are correct within 1 % as far as the hard radiation is concerned.

If there is an excited electron e^*, it can be produced in the process e^+e^- -> ee^* and it will subsequently decay into $e\gamma$. The $e^\pm\gamma$ invariant mass distribution shown in Fig.4-a displays no evidence for such an excited electron, allowing us to set an upper limit on its production cross section in the available mass range. The bump around 12 GeV/c^2 in Fig.4-a reflects the kinematical effects of the cuts on the opening angle and the lowest shower cluster energy. The interaction Lagrangian of a spin-1/2 excited lepton can be written as/12/

$$L_{int.} = \frac{\lambda e}{M} \bar{l}\, \sigma_{\mu\nu}\, l^*\, F^{\mu\nu} + \text{h.c.} .$$

The production cross section for $e^+e^- \to e^{*+}e^-$ is then given by/12/,

$$\frac{d\sigma}{d\Omega} = -\frac{2\pi\alpha^2\lambda^2}{M^2 s}\left[\frac{t^2+(t-M^2)^2}{s} + \frac{s^2+(s-M^2)^2}{t}\right],$$

where λ is the coupling constant of e^* to $e\gamma$, M is the mass of e^* and t is the square of the 4-momentum transfer between the initial positron and the produced e^{*+}.

The 95 % CL upper limit for the coupling constant λ is shown in Fig. 4-b as a function of the e^* mass M. The existence of such an excited electron state would also have an effect on the reaction $e^+e^- \to \gamma\gamma$, the cut-off parameter $\Lambda+$ being related to λ and M by the relationship $M^2/\lambda = \Lambda^2+ /6/$; the resulting upper limit curve for λ is also shown as a function of M in Fig. 4-b. The $e^+e^-\gamma$ analysis gives a much more restrictive upper limit on λ for M less than 34 GeV/c^2.

In summary, we have measured the cross sections of the reactions e^+e^- -> e^+e^- and $\gamma\gamma$. They show good agreement with the QED predictions and the cut-off parameters for both reactions have been determined. The

electro-weak effects were studied in Bhabha scattering and the results are consistent with the standard model. The higher order QED processes e^+e^- -> $e^+e^-\gamma$ and $\gamma\gamma\gamma$ were also studied and the results agree with the QED predictions of order α^3. In the $e^+e^-\gamma$ events, no indication of an excited electron was observed in the invariant mass plot of the system consisting of electron/positron and photon, yielding new limits on the coupling constant λ in the mass range between 1 and 34 GeV/c^2.

We are indebted to the PETRA machine group for their excellent support during the experiment and to all the engineers and technicians of the collaborating institutions who have participated in the construction and maintenance of the apparatus. This experiment was supported by the Bundesministerium für Forschung und Technologie, by the Education Ministry of Japan and by the UK Science and Engineering Research Council through the Rutherford Appleton Laboratory. The visiting groups at DESY wish to thank the DESY directorate for their hospitality.

Figure Captions

Fig.1

a Integrated cross sections for the reaction $e^+e^- \to \gamma\gamma$ in the region $|\cos\vartheta| \leq 0.76$ for c.m. energies between 12 GeV and 34.6 GeV. The curve is the QED expectation.

b Differential cross sections for the reaction $e^+e^- \to \gamma\gamma$ for c.m. energies 14.0, 22.0 and 34.6 GeV. The lines show the QED expectations.

c The ratio of the measured differential cross section to the lowest order QED prediction for the reaction $e^+e^- \to \gamma\gamma$. The solid curves show the expectations with the cut-off parameters $\Lambda\pm$ = 50 and 60 GeV.

Fig.2

a Integrated cross sections for the reaction $e^+e^- \to e^+e^-$ in the region $|\cos\vartheta| \leq 0.76$ for c.m. energies between 12 GeV and 34.6 GeV. The curve is the QED expectation.

b Differential cross sections for the reaction $e^+e^- \to e^+e^-$ for c.m. energies 14, 22 and 34.6 GeV. The lines show the QED expectations.

c The ratio of the measured differential cross section for the reaction $e^+e^- \to e^+e^-$ to the lowest order QED prediction. The solid curve shows the expectation from the standard electro-weak theory with $\sin^2\vartheta_w = 0.26$.

Fig.3

a Photon energy distribution for the reaction $e^+e^- \to \gamma\gamma\gamma$, normalised to the beam energy.

b Opening angle distribution between any two photons for the reaction $e^+e^- \to \gamma\gamma\gamma$.

c Photon energy distribution for the reaction $e^+e^- \to e^+e^-\gamma$, normalised to the beam energy.

d Opening angle distribution between electron and positron for the reaction $e^+e^- \to e^+e^-\gamma$.

The histograms show the predictions of the order α^3 QED.

Fig.4

a Invariant mass distribution of the $(e^\pm\gamma)$ system in the reaction $e^+e^- \to e^+e^-\gamma$ (2 entries / event). The histogram shows the prediction of the order α^3 QED.

b The 95 % confidence level upper limit for the coupling constant λ as a function of the excited electron mass M. These results are obtained from Fig.4-a. The smooth curve shows the 95 % confidence level upper limit on λ obtained from the reaction $e^+e^- \to \gamma\gamma$.

References

1. JADE Collab., W. Bartel et al., Phys. Lett. 92B(1980)206;
   Phys. Lett. 99B(1981)281.

2. MARK-J Collab., D.P. Barber et al., Phys. Rev. Lett. 43(1979)1915;
   Phys. Rev. Lett. 46(1981)1663.
   PLUTO Collab., Ch. Berger et al., Z. Physik C4(1980)269;
   Phys. Lett. 94B(1980)87.
   TASSO Collab., R. Brandelik et al., Phys. Lett. 94B(1980)259;
   Phys. Lett. 117B(1982)365.
   CELLO Collab., H.J. Berend et al., Phys. Lett. 103B(1981)148;
   Phys. Lett. 123B(1983)127.

3. JADE Collab., W. Bartel et al., Phys. Lett. 88B(1979)171.

4. Monte Carlo generation for $e^+e^- \to$ hadrons
   B. Andersson, G. Gustafson and T. Sjöstrand,
   Phys. Lett. 94B(1980)211, and the earlier references therein,
   for details, see ; T. Sjöstrand, LUTP 80-3 (April 1980) and
   Errata to LUTP 80-3.

5. Monte Carlo generation for $e^+e^- \to \tau^+\tau^-$ and e^+e^- followed
   F.A. Berends et al., Nucl. Phys. 57B(1973)381
   61B(1973)414
   63B(1973)381
   68B(1974)541
   177B(1981)237
   F.A. Berends and G.J. Komen, Phys. Lett. 63B(1976)432

6. A. Litke, Harvard Univ., Ph. D. Thesis(1970) unpublished.

7. S.D. Drell, Ann. Phys. 4(1958)75
T.D. Lee and G.C. Wick, Nucl. Phys. B9(1969)209.
It should be noted that $\Lambda\pm$ were defined in a different way in ref. 1.

8. Particle Data Group, Rev. Mod. Phys. 52(1980) No.2, Part II.

9. R. Budny, Phys. Lett. 55B(1975)227

10. V. Barger et al., Phys. Rev. D22(1980) 727

11. E.H. de Groot et al.,Phys. Lett. 90B(1980)427; 95B(1980)128

12. H. Terazawa et al., INS-Rep.-443 Dec 1981, University of Tokyo.

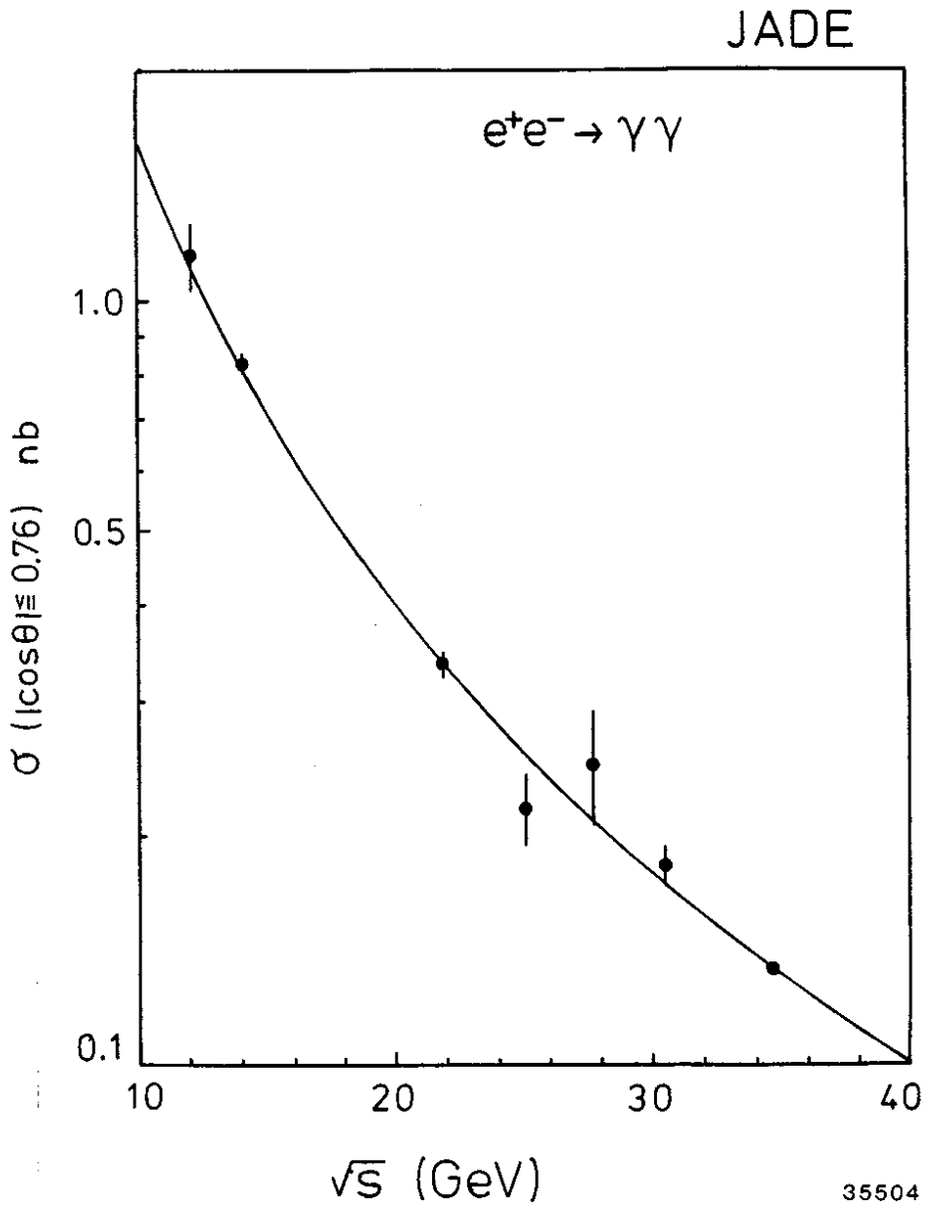

Fig. 1a

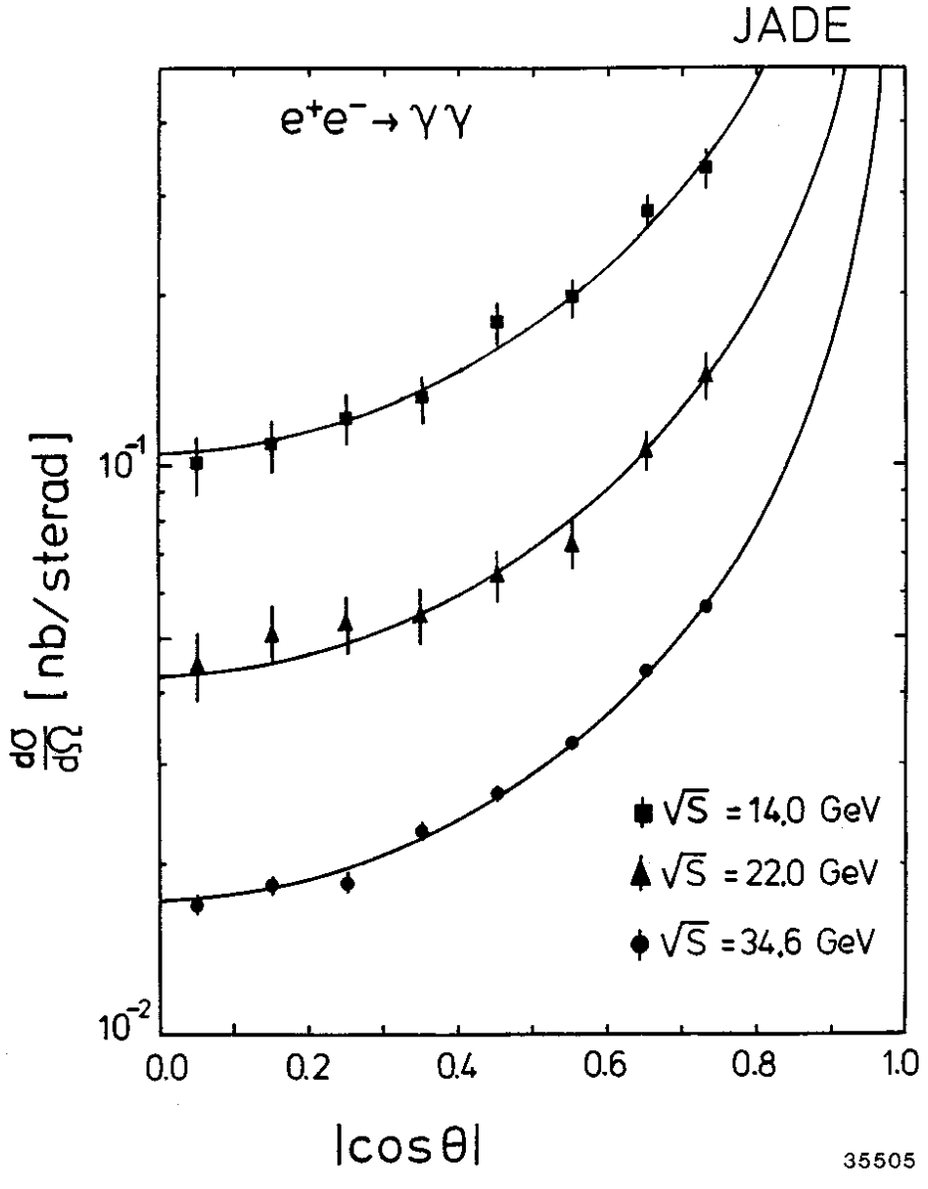
JADE
$e^+e^- \to \gamma\gamma$
$\frac{d\sigma}{d\Omega}$ [nb/sterad]
10^{-1}
10^{-2}
$\sqrt{s}$ = 14.0 GeV
$\sqrt{s}$ = 22.0 GeV
$\sqrt{s}$ = 34.6 GeV
0.0
0.2
0.4
0.6
0.8
1.0
|cos θ|
35505

Fig. 1b

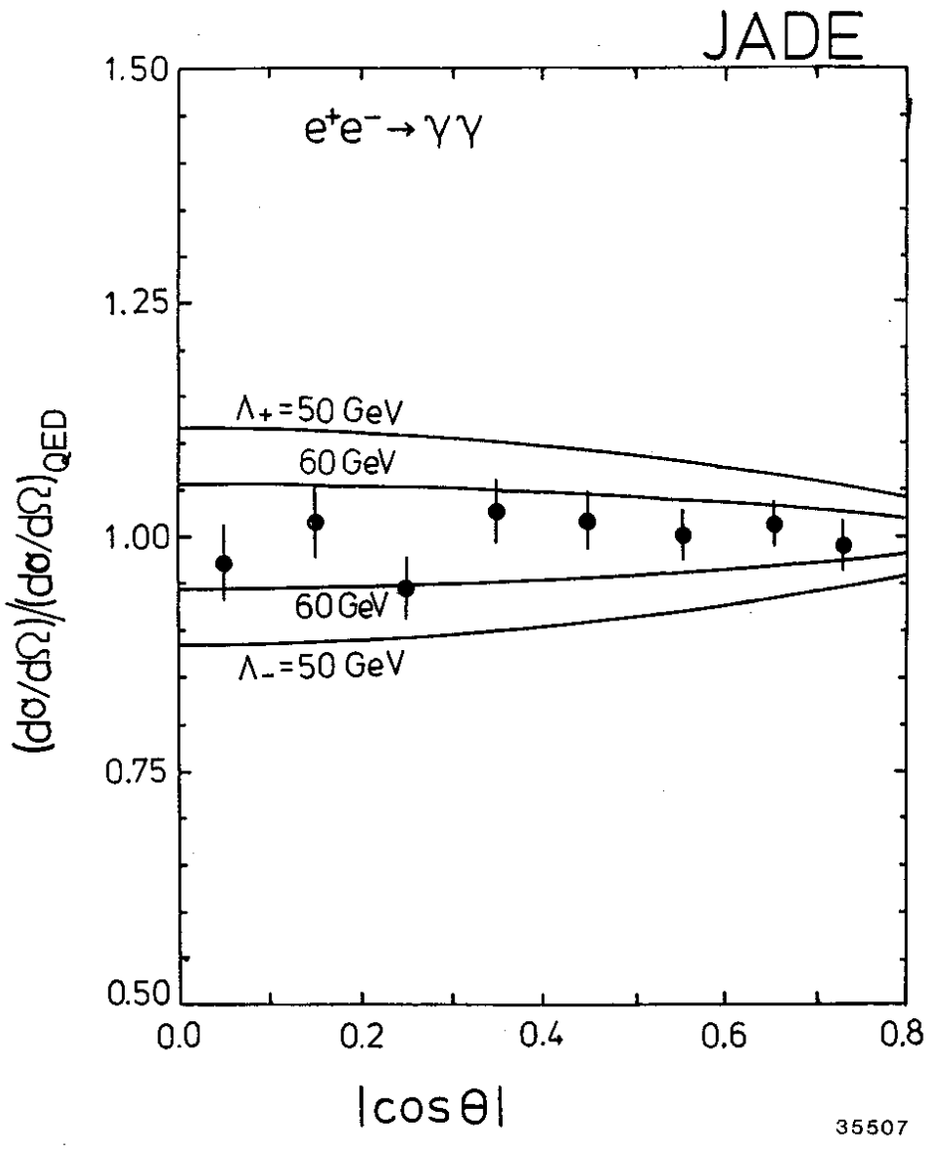
JADE
$e^+e^- \to \gamma\gamma$
$(d\sigma/d\Omega)/(d\sigma/d\Omega)_{QED}$
1.50
1.25
1.00
0.75
0.50
Λ_+ = 50 GeV
60 GeV
60 GeV
Λ_- = 50 GeV
0.0
0.2
0.4
0.6
0.8
|cos θ|
35507

Fig. 1c

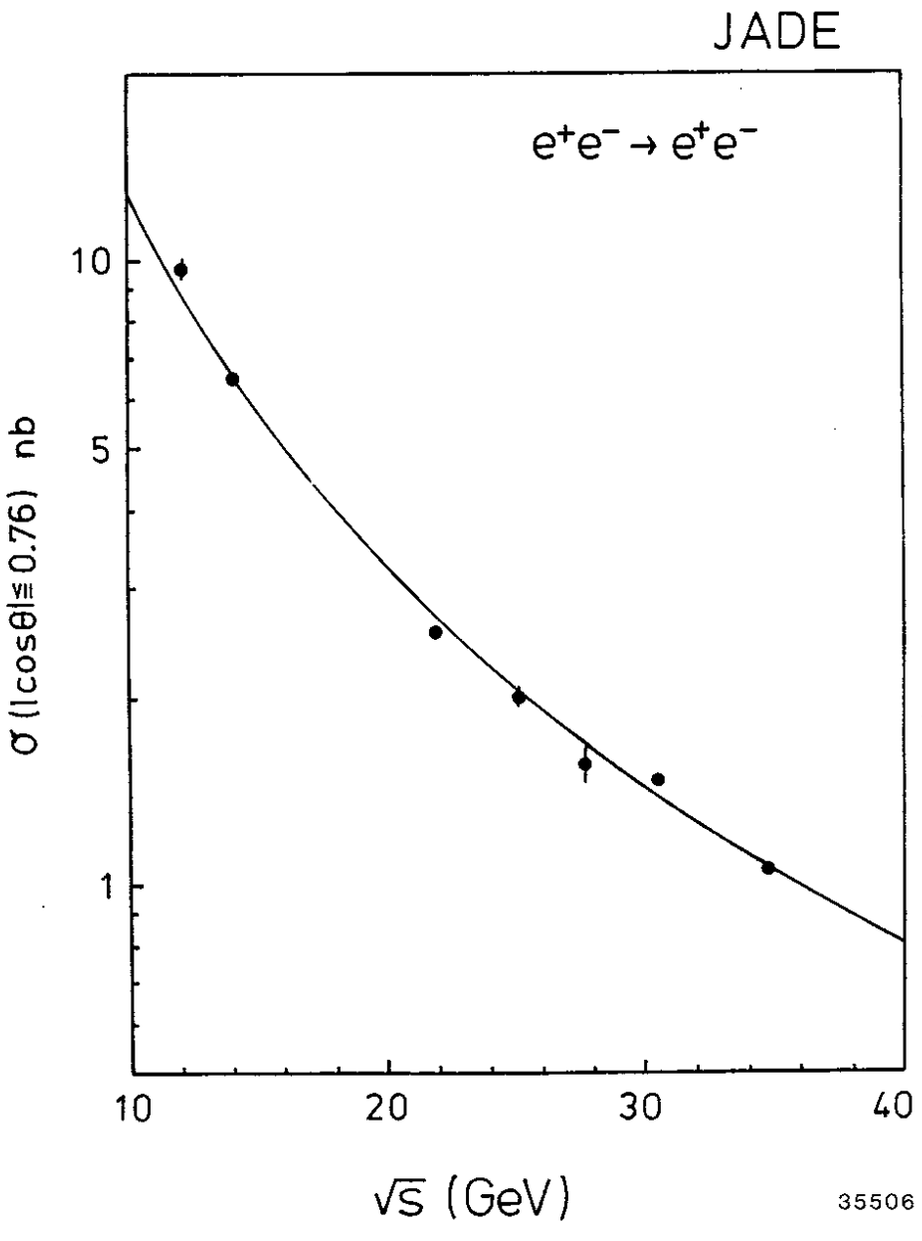
JADE
$e^+e^- \to e^+e^-$
σ ($|\cos\theta| \leq 0.76$) nb
10
5
1
10
20
30
40
$\sqrt{s}$ (GeV)
35506

Fig. 2a

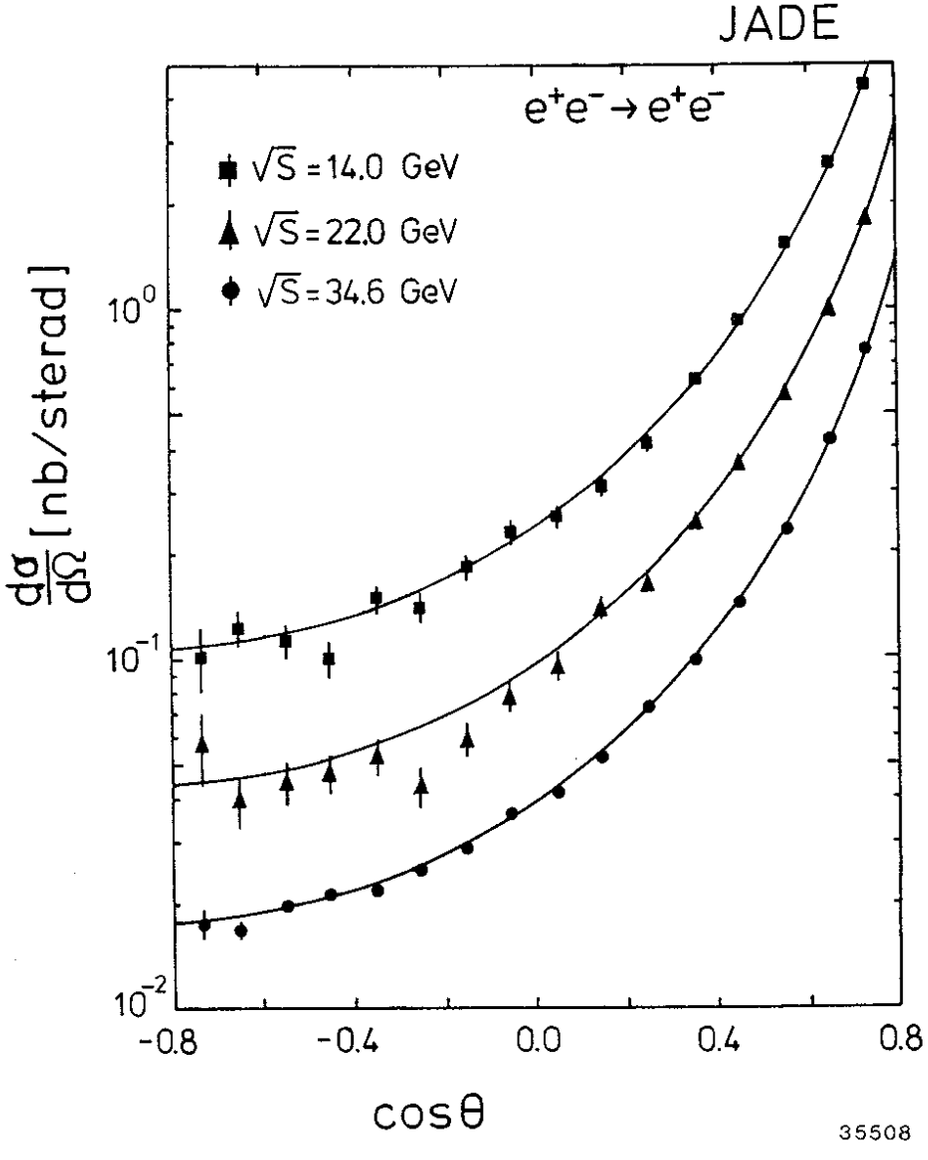
JADE
$e^+e^- \to e^+e^-$
$\sqrt{S}$ = 14.0 GeV
$\sqrt{S}$ = 22.0 GeV
$\sqrt{S}$ = 34.6 GeV
$\frac{d\sigma}{d\Omega}$ [nb/sterad]
10^0
10^{-1}
10^{-2}
-0.8
-0.4
0.0
0.4
0.8
cosθ
35508

Fig. 2b

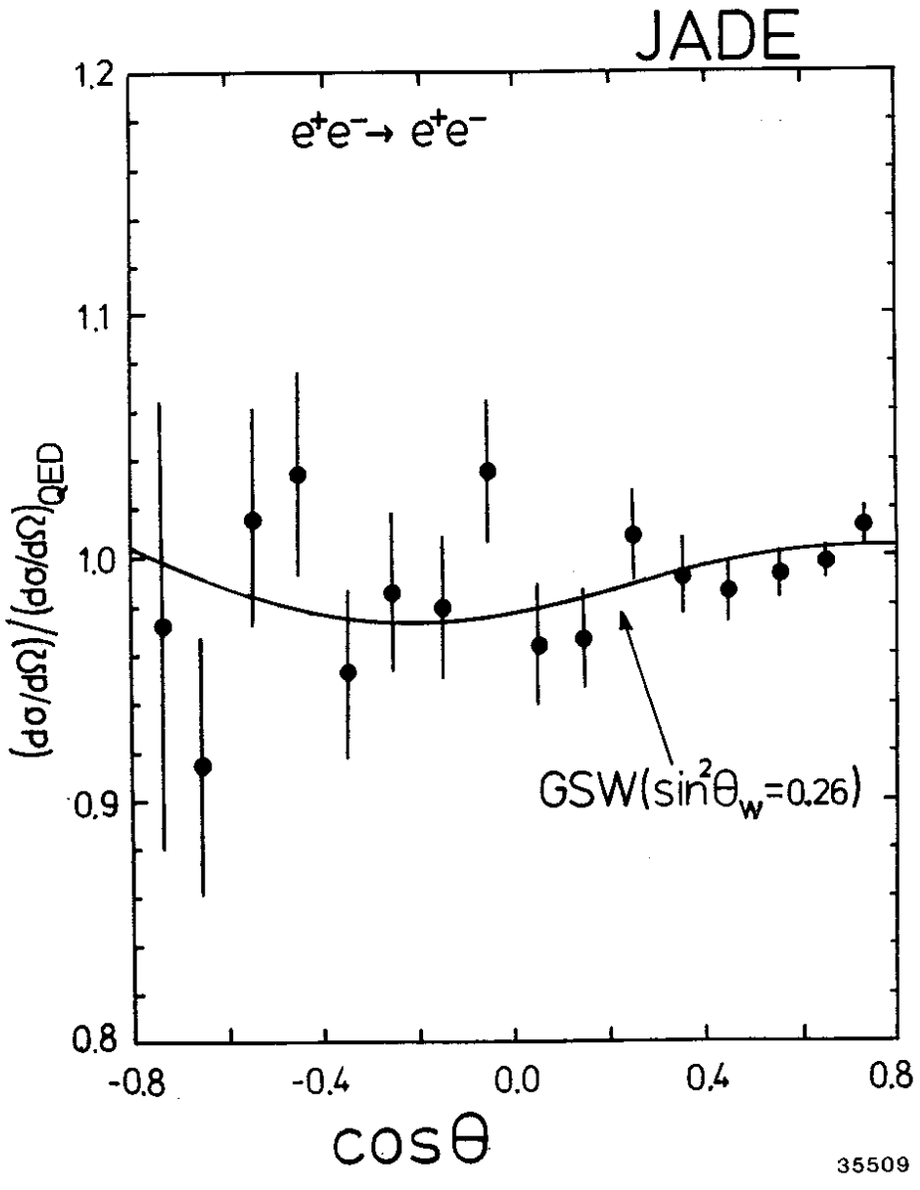
JADE
$e^+e^- \rightarrow e^+e^-$
$(d\sigma/d\Omega)/(d\sigma/d\Omega)_{QED}$
GSW($\sin^2\theta_w$=0.26)
cosθ
35509

Fig. 2c

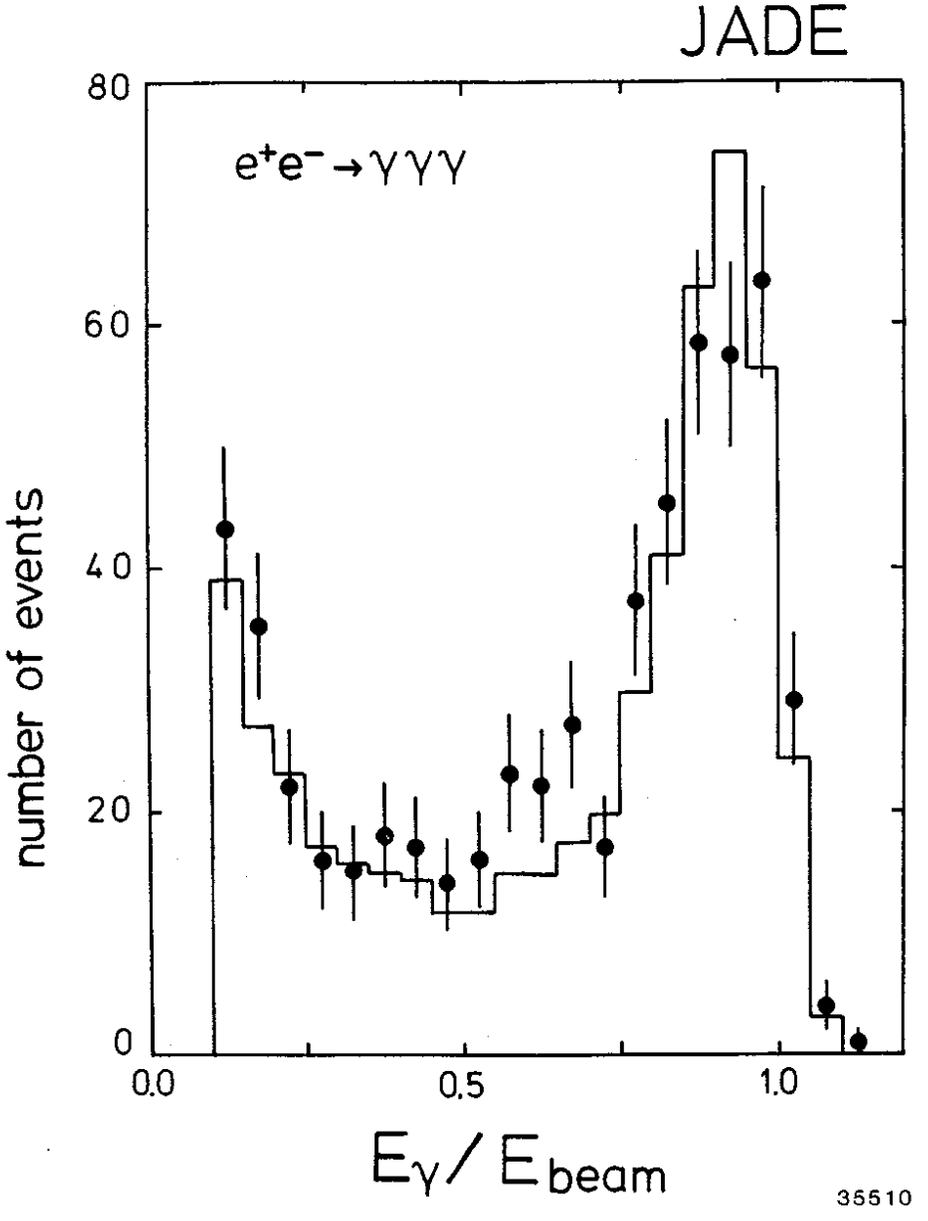
JADE
$e^+e^- \rightarrow \gamma\gamma\gamma$
number of events
E_γ / E_{beam}
35510

Fig. 3a

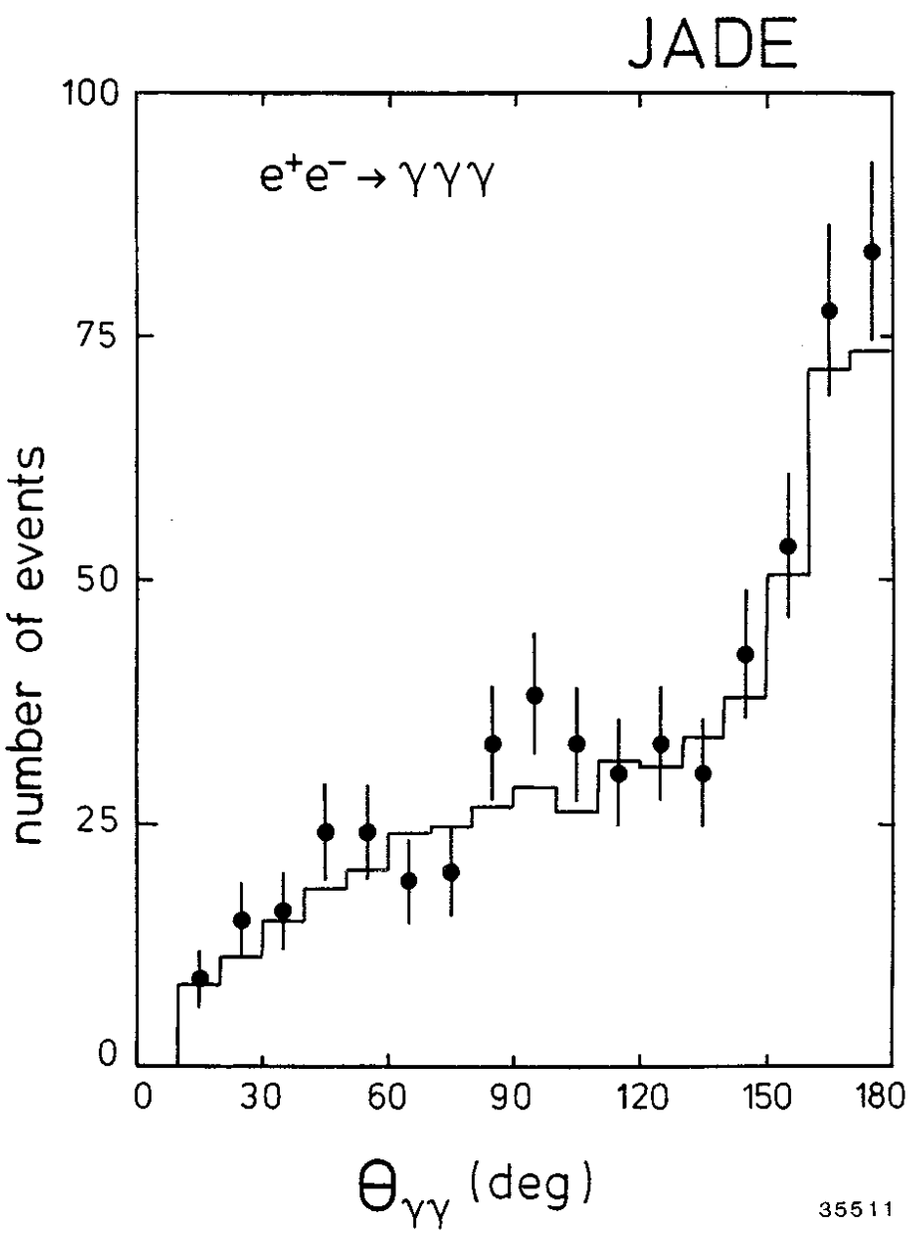
JADE
$e^+e^- \to \gamma\gamma\gamma$
number of events
100
75
50
25
0
0
30
60
90
120
150
180
$\Theta_{\gamma\gamma}$ (deg)
35511

Fig. 3b

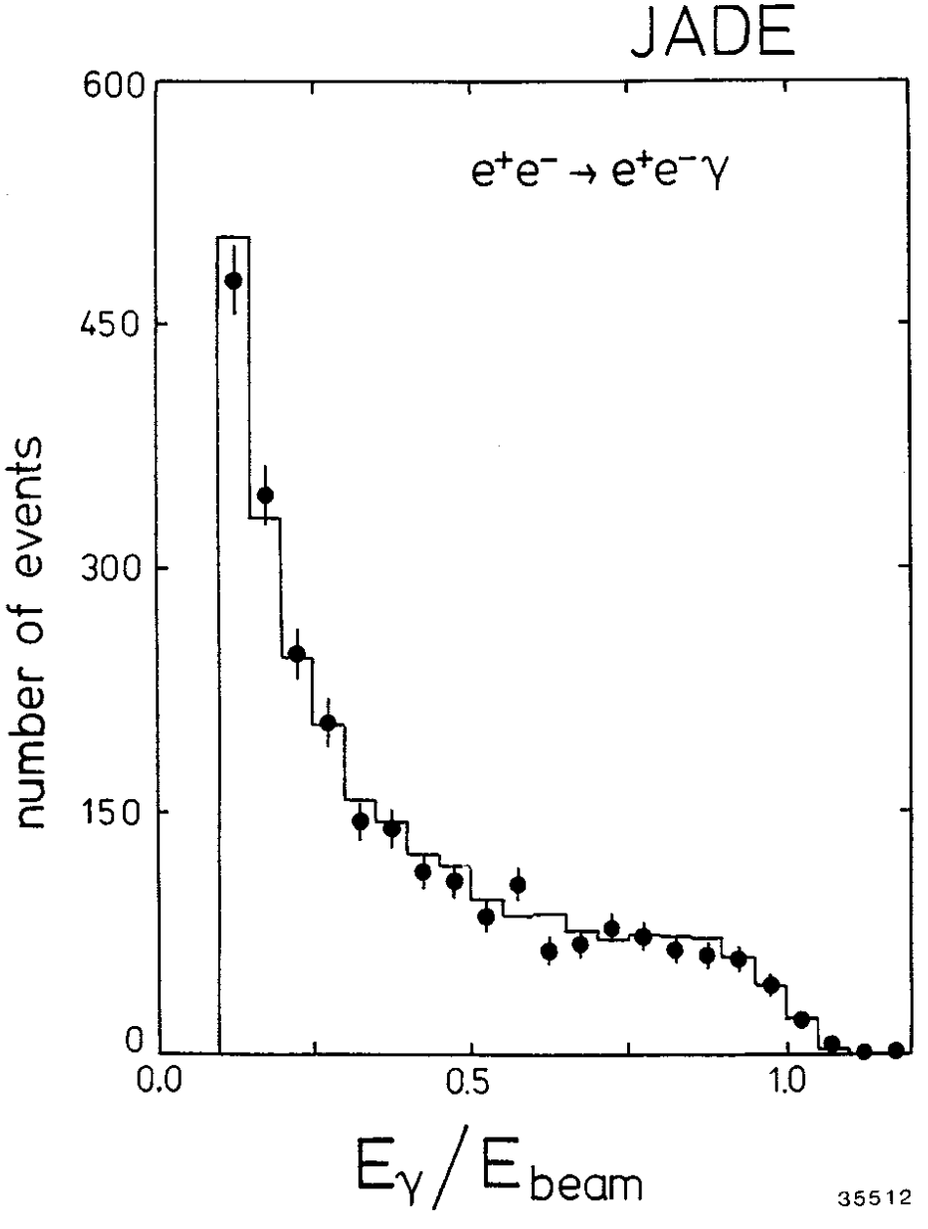
JADE
$e^+e^- \to e^+e^-\gamma$
number of events
600
450
300
150
0
0.0
0.5
1.0
E_γ / E_{beam}
35512

Fig. 3c

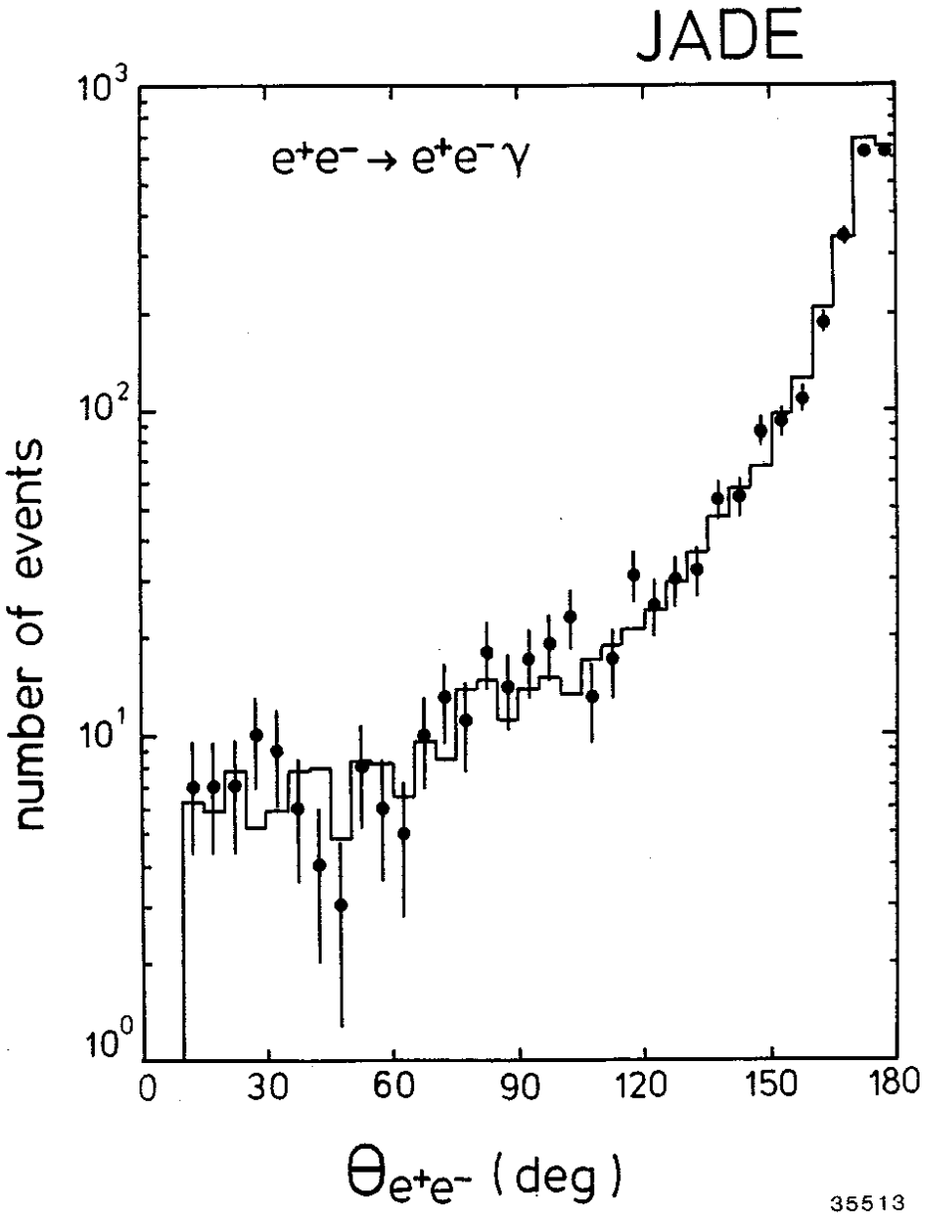
JADE
$e^+e^- \to e^+e^-\gamma$
number of events
10^3
10^2
10^1
10^0
0
30
60
90
120
150
180
$\Theta_{e^+e^-}$ (deg)
35513

Fig. 3d

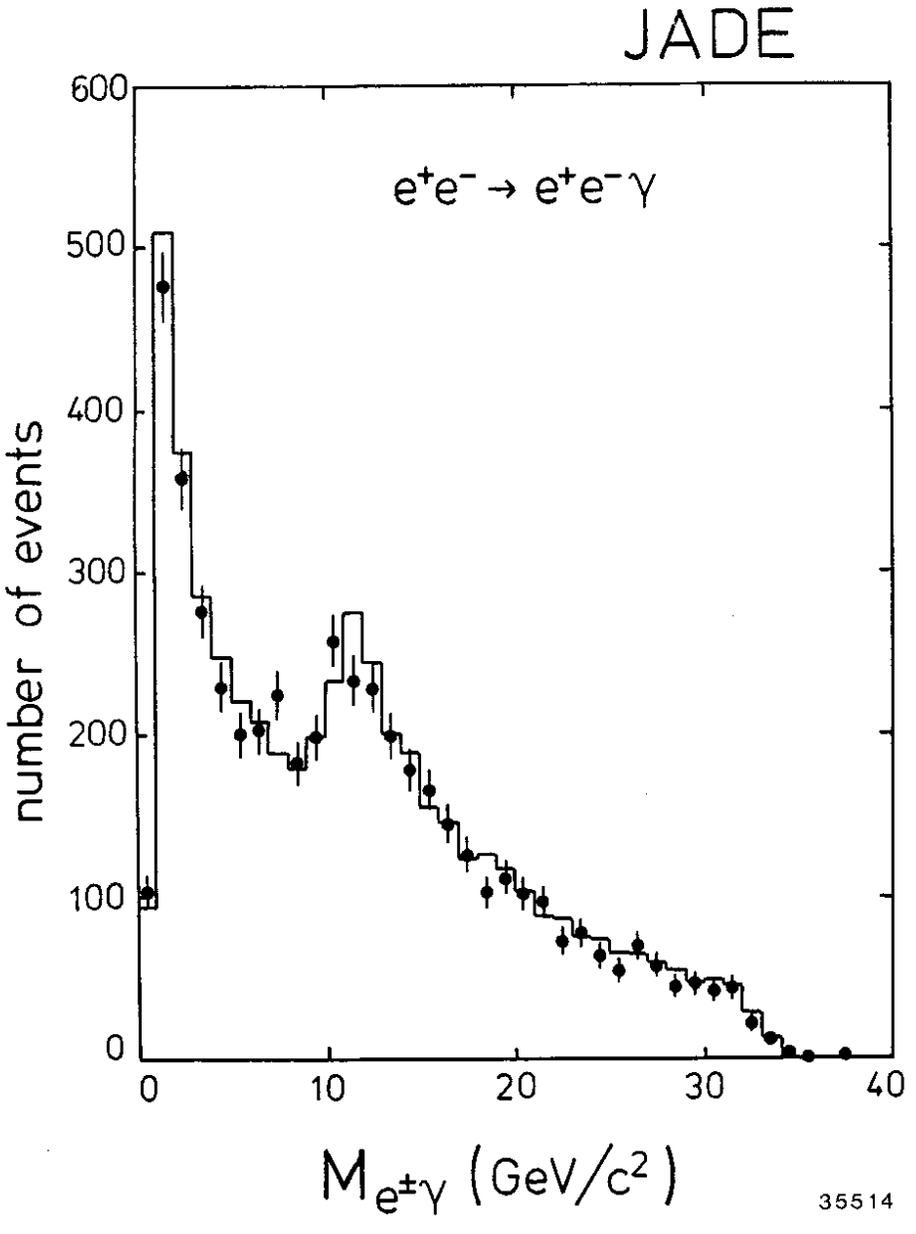
JADE
$e^+e^- \to e^+e^-\gamma$
number of events
600
500
400
300
200
100
0
0
10
20
30
40
$M_{e^\pm\gamma}$ (GeV/c^2)
35514

Fig. 4a

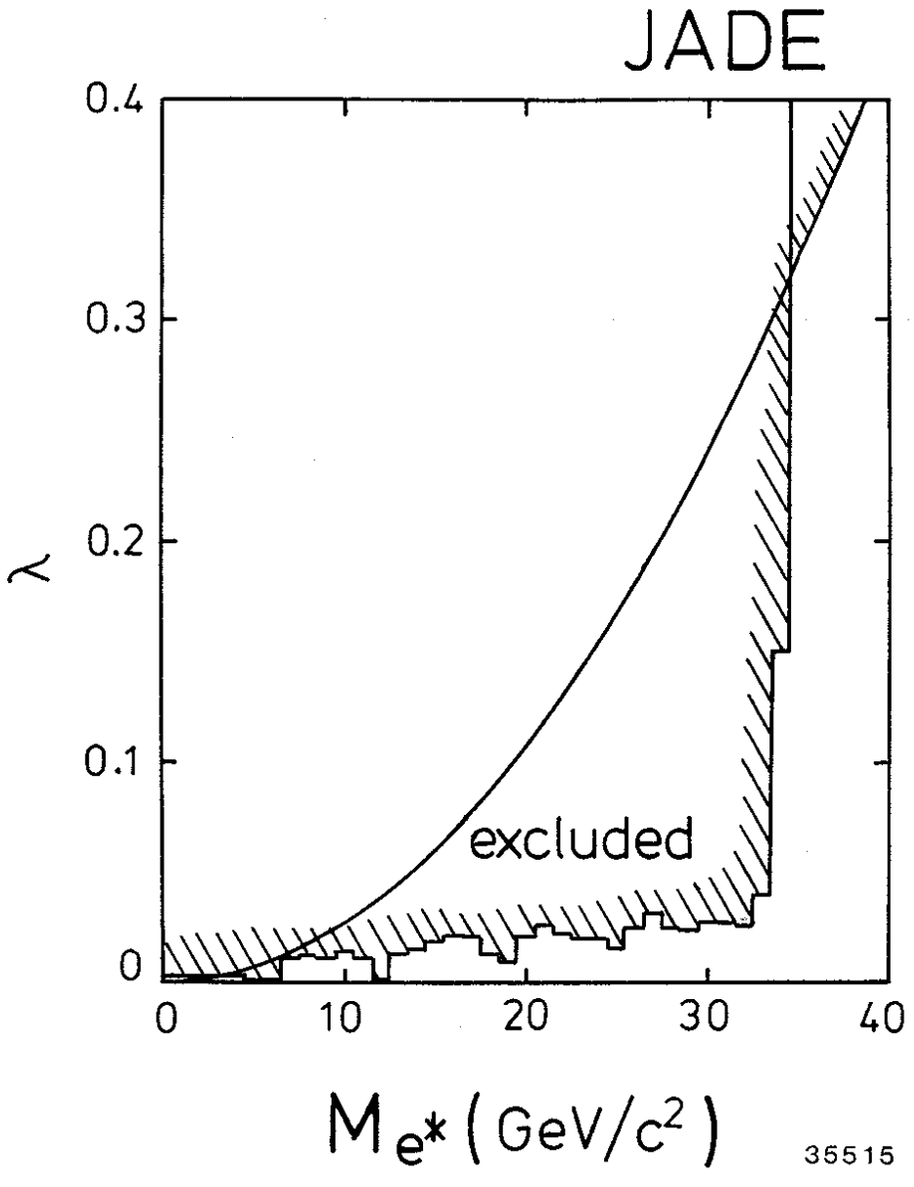

Fig. 4b